Phase Equilibrium Study of ZnO-"FeO"-SiO_2 System at Fixed Po_2 10^{-8} atm

HONGQUAN LIU, ZHIXIANG CUI, MAO CHEN, and BAOJUN ZHAO

Experimental studies of phase equilibria and liquidus temperatures have been carried out in the systems "FeO"-SiO_2 and ZnO-"FeO"-SiO_2 at Po_2 10^{-8} atm. Research techniques have been developed to enable the ZnO-containing system to be investigated under reducing conditions controlled by CO-CO_2 gas mixture. The experimental approach includes master slag preparation, high-temperature equilibration, quench, and electron probe X-ray microanalysis (EPMA). Phase compositions in the quenched samples were measured by EPMA and used for construction of phase diagram. It was found that the isotherms of the system ZnO-"FeO"-SiO_2 at Po_2 10^{-8} atm are significantly different from those in equilibrium with metallic iron and those predicted by FactSage. The presence of ZnO in copper smelting slag significantly increases the liquidus temperature in spinel primary phase field. Partitioning of ZnO in liquid and spinel is also discussed in this paper.

DOI: 10.1007/s11663-015-0480-1

I. INTRODUCTION

PYROMETALLURGICAL process continues to be the principal technology in copper production which include smelting, converting, and refining.[1] The objective of the smelting is to partially oxidize sulfur and iron from the Cu-Fe-S concentrate to produce a Cu-enrich molten sulfide phase (matte). Simultaneously, the gangue components in the concentrate form the molten slag by reacting with added flux (SiO_2). Slag properties play critical roles in the copper production, which closely related to metal recovery, slag tapping, and refractory corrosions under operating conditions.[2] Currently, approximately, 50 pct copper concentrate smelting is carried out by bath smelting furnaces that include top-blown (Ausmelt and Isasmelt), side-blown (Noranda and Teniente), and recently developed bottom-blown technologies.[3] The first commercial bottom-blown oxygen copper smelting furnace (BBF) at Dongying Fangyuan Nonferrous Metals Co., Ltd has shown excellent performance and drawn significant interest.[3–5] However, as a new copper smelting technology, the knowledge of thermodynamics and physic-chemistry in this smelting process is limited, and current research is part of the comprehensive research program to narrow the knowledge gap. A detailed analyses[3] on BBF slag compositions showed that in addition to the major components "FeO" (both Fe^{2+} and Fe^{3+}), and SiO_2, significant amount of ZnO is also present, and spinel is the primary phase present under the BBF smelting condition in which the oxygen partial pressure (Po_2) was estimated to be 10^{-8} atm.

Phase equilibria of ZnO-SiO_2 system have been well determined by a number of studies.[6,7] The first study on this system was reported by Bunting[7] which did not consider the loss of zinc at high temperatures. A reinvestigation on this system was conducted by Hansson *et al.*[6] using equilibration and quenching followed by EPMA analysis approach. Sub-solidus studies on the Fe-Zn-O system were systematically conducted by Hansson *et al.*[8–10] under air and intermediate Po_2, while the experiments under metallic iron saturation on the same system were conducted at 1100 K (827 °C) by Itoh *et al.*[11] using EMF method. Phase equilibria studies on Fe-Zn-O system were also carried out by Itoh and Azakami[12,13] at 1100 K and 1200 K (827 °C and 927 °C) in closed quartz capsule where the oxygen partial pressure was determined to be in a wide range 10^{-3} to 10^{-20} atm.

As a base of the copper smelting slags, the pseudo-binary "FeO"-SiO_2 system has been extensively studied under different conditions including metallic iron saturation,[14] air atmosphere,[15,16] and the intermediate Po_2.[16–18] Significant differences on the liquidus temperatures and primary phase fields were observed under various equilibration conditions.

Previous studies in Fe-O-ZnO-SiO_2 system have been focused in air[19] and at metallic iron saturation.[19–22] No information was found in this system relevant to the copper smelting conditions around Po_2 10^{-8} atm. In order to evaluate the effect of the ZnO content on phase equilibria of the copper smelting slags, present study is focused on the phase equilibria of ZnO-"FeO"-SiO_2 system at Po_2 10^{-8} atm.

II. EXPERIMENTAL METHODOLOGY

Experimental techniques used in present research are similar to that described in previous papers.[23,24] Briefly,

HONGQUAN LIU, Ph.D. Student, MAO CHEN, Postdoctoral Research Fellow, and BAOJUN ZHAO, Codelco-Fangyuan Professor, are with The University of Queensland, Brisbane, Australia. Contact e-mail: baojun@uq.edu.au ZHIXIANG CUI, President, is with Dongying Fangyuan Nonferrous Metals Co., Ltd., Dongying, China.

Manuscript submitted May 29, 2015.
Article published online October 20, 2015.

the sample was directly quenched into ice water after the equilibration at controlled temperatures and Po_2 10^{-8} atm, followed by EPMA analysis to determine the phase assemblages and composition of each phase present. However, in the present study, the oxygen partial pressure of the slag was controlled by the CO-CO_2 gas mixture, and the bulk composition of the slag could be changed during the equilibration due to the vaporization of zinc. As a first study in the system ZnO-"FeO"-SiO_2 system at Po_2 10^{-8} atm, the research technique has been further developed.

A. *Sample and Substrate Preparation*

The oxygen partial pressure of the slag was controlled by the CO-CO_2 gas mixture, and the reactions between liquid slag and gas are relatively slow. Long reaction time at given temperature is required to achieve equilibrium. On the other hand, zinc oxide in the slag could be reduced, and zinc metal will vaporize from the slag. To ensure the final equilibrium can be achieved in the controlled time and to reduce the vaporization of zinc, master slags have been prepared in the conditions close to the temperature and oxygen partial pressure required for the final equilibration.

Approximately, 0.1 g pelletized mixture was used in each experiment. The mixtures were prepared by mixing the desired amounts of iron silicate master slag and zinc silicate master slag with additional "FeO," ZnO, or SiO_2. The "FeO" was prepared from iron foil at the same temperature and oxygen partial pressure required for the final equilibration.

Two master slags, as shown in Table I, were prepared from high-purity ZnO, SiO_2, Fe_2O_3, and Fe (Table II). It can be seen from Figure 1, excess ZnO was always added in the starting mixture to compensate the loss of ZnO during the equilibration. All the iron oxides used in the present study were pre-conditioned according to the target equilibrium conditions to ensure the equilibrium to be attained. The compositions of the phases were measured by EPMA after the equilibration so that the changes in bulk composition during high-temperature equilibration do not affect the phase diagrams to be constructed.

In order to increase the reaction rate between slag and gas and the cooling rate after the equilibration, the substrates made from quartz (SiO_2)[23] and spinel (Fe_3O_4)[25] were used to hold the mixtures for the experiments targeted in the SiO_2 and spinel primary phases, respectively. Pt baskets were used as a container to determine the liquidus in willemite primary phase field. It should be noted that the small amount of iron may be dissolved into Pt wire, and the bulk composition of the slag could change.[26,27]

B. *Equilibration*

Equilibration experiments were carried out in a vertical reaction tube furnace. A working thermocouple protected by a recrystallized alumina sheath was placed inside the reaction tube to monitor the actual temperature of the sample. The working thermocouple was periodically calibrated against a standard thermocouple (supplied by the National Measurement Institute of Australia, NSW, Australia). The overall absolute temperature uncertainty was estimated to be ±3 K (±3 °C).

Mixtures of CO-CO_2 gases at different CO/CO_2 ratios were used to obtain the required oxygen partial pressure 10^{-8} atm. The oxygen partial pressures at different temperatures were confirmed by the yttria-stabilized zirconia solid electrolyte cell oxygen probe ($SIRO_2$, DS-type oxygen probe; Australian Oxytrol Systems, Victoria, Australia). The results of the measurements were within the accuracy of the DS-type oxygen probe, *i.e.*, ±0.1 log (Po_2) unit,[28] details as shown in Table III.

Table II. Chemicals Used in the Present Study

Materials	Purity (pct)	Supplier
Iron foil (Fe)	99.5+	Goodfellow Cambridge Ltd.
Platinum foil (Pt)	99.9	Cookson Ltd.
SiO_2	99.9	Alfa Aesar
ZnO	99.9	Sigma Aldrich
Fe_2O_3	99.99	Alfa Aesar
Iron powder (Fe)	99.0	Goodfellow Cambridge Ltd.
CO	99.97	Coregas
CO_2	99.995	Coregas

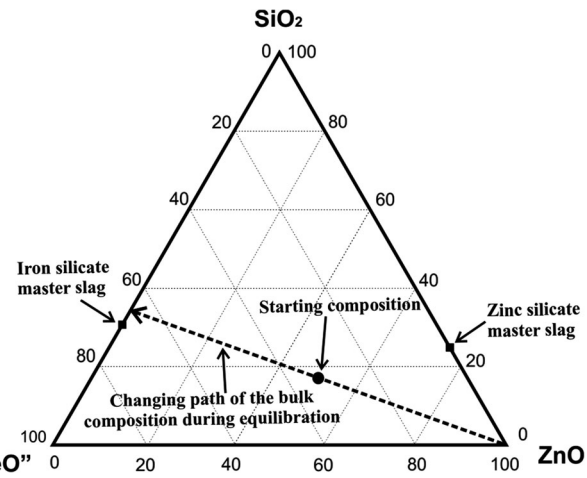

Fig. 1—Bulk composition changes during the equilibration of the "FeO"-ZnO-SiO_2 slags at Po_2 10^{-8} atm.

Table I. Master Slags Used in Current Research

Master Slag	Temperature	Po_2 (atm)	Time (h)	Composition (wt pct) ZnO	SiO_2	"FeO"
Zinc silicate	1773 K (1500 °C)	0.21	0.5	74.4	25.6	0.0
Iron silicate	same as final equilibration temperature	10^{-8}	16	0.0	33.0	67.0

Table III. Gas Ratios in Current Study at Varied Temperatures and the Calibration Results

Temperature [K (°C)]	Flow Rate (ml/min)		Log (Po_2)	
	CO_2	CO	Theoretical	Calibration
1443 (1170)	400.0	7.9	−8.0	−7.9
1473 (1200)	400.0	12.7	−8.0	−7.9
1493 (1220)	400.0	17.2	−8.0	−8.0
1523 (1250)	400.0	26.9	−8.0	−8.0
1543 (1270)	400.0	35.8	−8.0	−8.0
1573 (1300)	400.0	54.3	−8.0	−8.0

The sample was introduced from the bottom of the reaction tube and held at the cold zone with flush of gas mixture for 15 to 30 minutes to remove the air. The sample was then raised and kept in the hot zone of the reaction tube for required period.

After the equilibration, the bottom of the reaction tube was immersed in ice water and the lid was removed. Then, the sample was dropped directly into the water by pulling up the iron wire which suspended the sample. The quenched sample was dried on a hot plate, mounted in epoxy resin, and polished for metallographic examinations.

C. *Sample Analysis*

The polished samples were first examined with optical microscopy to observe the phases present and then coated with carbon using QT150TES (Quorum Technologies) Carbon Coater for electron microscopic analyses. A JXA 8200 electron probe X-ray microanalyzer (EPMA) with wavelength dispersive detectors was used for microstructure and composition analyses. The analyses were conducted with an accelerating voltage of 15 kV and a probe current of 15 nA. The standards used for analysis were from Charles M. Taylor Co. (Stanford, CA): Fe_2O_3 for Fe and $CaSiO_3$ for Si; and from Micro-Analysis Consultants Ltd. (Cambridge, UK): ZnO for Zn. The ZAF correction procedure supplied with the EPMA was applied. The overall accuracy of EPMA measurements is determined by precision and accuracy. Precision refers to the reproducibility of the measurements—and thus the ability to be able to compare compositions, whether within a sample, or between samples, or between analytical sessions. It is a relative description. Accuracy refers the "truth" of the analysis, and is directly tied to the standards used and the matrix correction applied to the raw data, as well equipment conditions and parameter. It is an absolute description. The overall accuracy of EPMA quantitative error analysis is a combination of both. In the present study, the liquid phase was relatively hard to be quenched to a homogenous glass, and 10 to 20 points were usually measured from different areas for liquid. The composition of the solid phase was more stable during cooling and 3 to 5 points were usually measured. The compositions of the phases were the average of 10 to 20 measurements for liquid and 3 to 5 measurements for solid. The precision for each phase composition is stated by the standard deviation which is usually below 1 pct. The accuracy of the EPMA measurements is determined by comparing the measured concentration of each element with the given value for the standards. The difference is always controlled below 1 pct. The overall accuracy of the EPMA measurements including both precision and accuracy is within 1 wt pct. Both Fe^{2+} and Fe^{3+} are present in the quenched samples; however, only metal cation concentrations can be measured by EPMA. All iron was recalculated to FeO for presentation purpose only.

III. RESULTS AND DISCUSSIONS

A. *Experimental Results in "FeO"-SiO_2 System*

The experiments were first carried out for the base system "FeO"-SiO_2 at $Po_2 = 10^{-8}$ atm in temperature range between 1473 K and 1573 K (1200 °C and 1300 °C). It was found that wüstite, spinel, and tridymite are the primary phases in the composition range investigated. The typical microstructures of the quenched samples are shown in Figure 2, where the equilibrium of liquid phase with one or two solid phases is shown in Figures 2(a) through (d), respectively. The normalized compositions of the phases measured by EPMA are shown in Table IV. It can be seen that the solubilities of SiO_2 in the wüstite and spinel are less than 1 wt pct. The maximum solubility of "FeO" in the tridymite was determined to be 1.0 wt pct. The phase diagram of "FeO"-SiO_2 system constructed from the experimental data is shown in Figure 3. The peritectic point between wüstite and spinel primary phase fields was determined to be 1549 K ± 10 K (1276 °C ± 10 °C) at 17.8 wt pct SiO_2. The eutectic point between spinel and tridymite primary phase fields was determined to be 1473 K ± 3 K (1200 °C ± 3 °C) at 34.3 wt pct SiO_2 in the present study.

The comparisons between the present results and previous studies[16,17] and FactSage 6.2[29] calculations at Po_2 10^{-8} atm are also shown in Figure 3. It can be seen that the present results are in good agreement with the results from Hidayat[17] and are significantly different from Muan's results[16] and FactSage predictions in wüstite and spinel primary phase fields.

"FeO"-SiO_2 is a base system for copper smelting slag, and phase diagram of this system measured at metallic iron saturation[21] has been used for long time to characterize the copper smelting slags. A comparison of present study with that under metallic iron saturation is shown in Figure 4. It can be seen that the fayalite (Fe_2SiO_4) primary

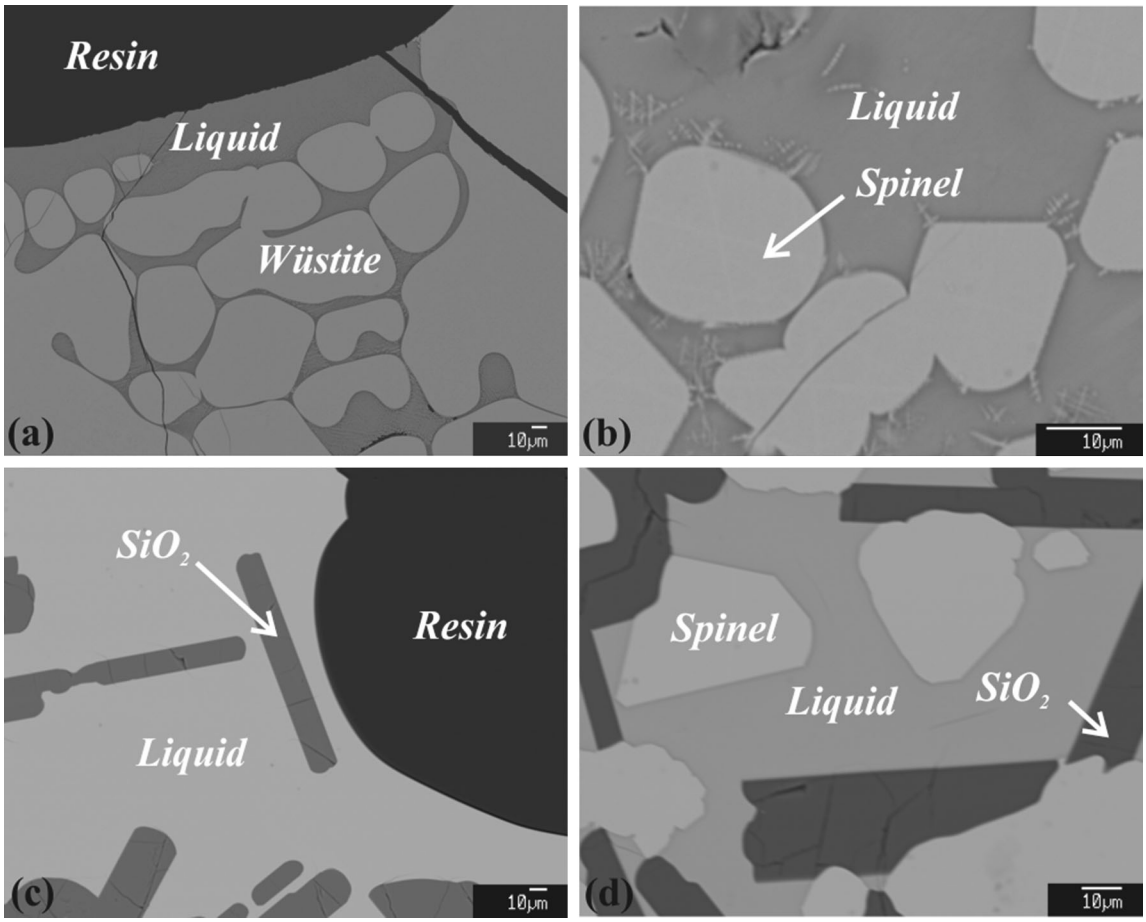

Fig. 2—Typical microstructures of quenched samples showing equilibrium of liquid with (*a*) wüstite—1573 K (1300 °C); (*b*) spinel—1523 K (1250 °C); (*c*) tridymite—1543 K (1270 °C); and (*d*) spinel and tridymite—1473 K (1200 °C).

phase at iron saturation is replaced by spinel primary phase when Po_2 is fixed at 10^{-8} atm. The liquidus temperatures at Po_2 10^{-8} atm are generally higher than those at metallic iron saturation.[21] Up to 70 K, difference in liquidus temperature is observed for these two different conditions. The comparison indicates that primary phase fields and liquidus temperatures of the "FeO"-SiO_2 system can be significantly influenced by oxygen partial pressure. The phase diagram measured previously at iron saturation cannot be used to accurately predict the liquidus temperatures of copper smelting slags.

B. *Experimental Results in ZnO-"FeO"-SiO_2 System*

The liquidus temperatures in ZnO-SiO_2 binary system have been determined in air by different authors.[6, 7] The eutectic points between tridymite and willemite primary phase fields, and between willemite and zincite primary phase fields were reported[6] to be 1721 K ± 5 K (1448 °C ± 5 °C) at 59 wt pct ZnO and 1775 K ± 5 K (1502 °C ± 5 °C) at 76.8 wt pct ZnO, respectively. No experimental data were reported in ZnO-"FeO" system at $Po_2 = 10^{-8}$ atm. The invariant point between wüstite and zinc primary phase fields used in construction of the phase diagram was taken from FactSage 6.2 prediction.[29]

In the present study, the liquidus temperatures in the ZnO-"FeO"-SiO_2 system have been experimentally determined at Po_2 10^{-8} atm between 1473 K and 1573 K (1200 °C and 1300 °C) (Table V). The primary phase fields in this system include tridymite, spinel, wüstite, and willemite. The typical microstructures of the quenched samples are shown in Figure 5. Figure 5(a) shows equilibrium of liquid with spinel at 1573 K (1300 °C). In Figure 5(b), the liquid was in equilibrium with tridymite at 1543 K (1270 °C). Figure 5(c) shows the liquid was in equilibrium with willemite at 1573 K (1300 °C). In Figure 5(d), the liquid was in equilibrium with both spinel and tridymite at 1543 K (1270 °C). Figure 5(e) shows that the liquid was in equilibrium with spinel and willemite at 1543 K (1270 °C), and Figure 5(f) shows that the liquid was in equilibrium with both tridymite and willemite at 1543 K (1270 °C).

The phase diagram of ZnO-"FeO"-SiO_2 system at Po_2 10^{-8} atm constructed based on the experimental data is shown in Figure 6. The thick solid lines represent experimentally determined boundaries between primary phase fields, while the thick dash lines are hypothetical boundaries. The thin solid lines are experimentally determined isotherms. It should be noted that the spinel [$(Fe^{2+},Zn)O\cdot Fe_2^{3+}O_3$], wüstite [$(Fe^{2+},Zn)O$], and willemite [$(Zn,Fe^{2+})SiO_4$] are all present as solid solutions in the slag.

Comparisons of 1523 K (1250 °C) isotherms between the present study and FactSage 6.2[29] predictions at Po_2 10^{-8} atm are shown in Figure 7. The experimentally

Table IV. Experimentally Determined Phase Composition in the "FeO"-SiO_2 System at Po_2 10^{-8} atm

Experiment No.	Temperature [K (°C)]	Phase	Composition (Wt Pct) SiO_2	Composition (Wt Pct) "FeO"
8	1573 (1300)	liquid	15.7	84.3
		wüstite	0.5	99.5
35	1573 (1300)	liquid	15.8	84.2
		wüstite	0.5	99.5
84	1573 (1300)	liquid	15.7	84.3
		wüstite	0.6	99.4
90	1573 (1300)	liquid	15.9	84.1
		wüstite	0.5	99.5
197	1563 (1290)	liquid	13.8	83.2
		wüstite	0.7	99.3
137	1543 (1270)	liquid	20.7	79.3
		spinel	0.2	99.8
150	1543 (1270)	liquid	20.4	79.6
		spinel	0.7	99.3
156	1543 (1270)	liquid	20.7	79.3
		spinel	0.7	99.3
101	1523 (1250)	liquid	25.4	74.6
		spinel	0.3	99.7
201	1523 (1250)	liquid	25.1	74.9
		spinel	0.8	99.2
196	1493 (1220)	liquid	31.2	68.8
		spinel	0.8	99.2
21	1473 (1200)	liquid	34.3	65.7
		spinel	0.3	99.7
		SiO_2	99.0	1.0
129	1493 (1220)	liquid	34.8	65.2
		SiO_2	99.7	0.3
39	1523 (1250)	liquid	36.5	63.5
		SiO_2	99.1	0.9
66	1523 (1250)	liquid	36.0	64.0
		SiO_2	99.3	0.7
133	1543 (1270)	liquid	36.7	63.3
		SiO_2	99.2	0.8
138	1543 (1270)	liquid	36.5	63.5
		SiO_2	99.4	0.6
38	1573 (1300)	liquid	38.1	61.9
		SiO_2	99.0	1.0
40	1573 (1300)	liquid	37.9	62.1
		SiO_2	99.4	0.6

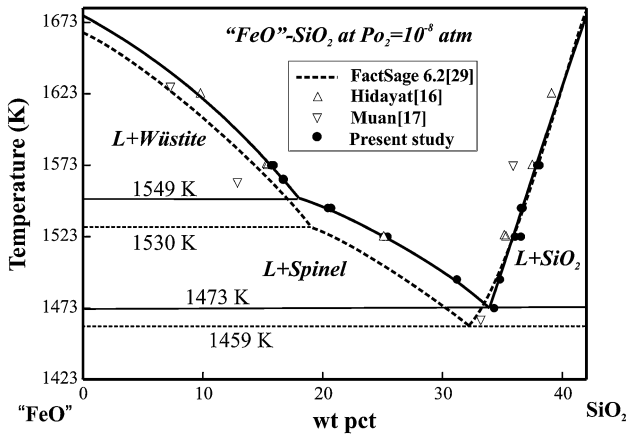

Fig. 3—Comparisons among the present and previous experimental results[16,17] and FactSage 6.2[29] predictions on "FeO"-SiO_2 system at Po_2 10^{-8} atm.

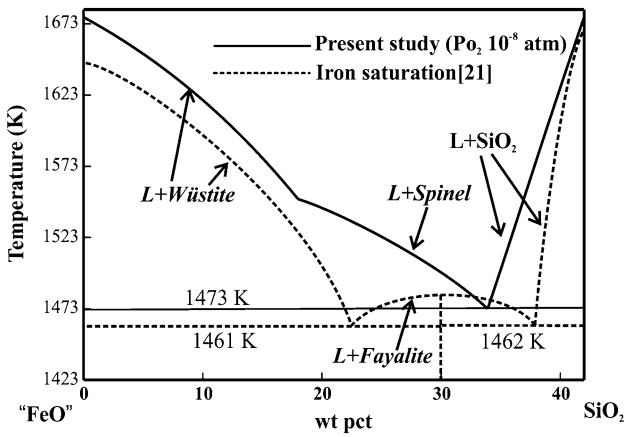

Fig. 4—Comparisons between the present study at Po_2 10^{-8} atm and the results at metallic iron saturation[21] on the system "FeO"-SiO_2.

Table V. Experimentally Determined Phase Compositions in the ZnO-"FeO"-SiO_2 System at Po_2 10^{-8} atm

Experiment No.	Temperature [K (°C)]	Phase	Composition (wt pct)		
			ZnO	SiO_2	"FeO"
10	1443 (1170)	SiO_2	0.1	98.8	1.1
		spinel	9.2	0.1	90.7
11	1443 (1170)	SiO_2	0.1	99.1	0.9
		spinel	8.0	0.3	91.6
12	1443 (1170)	SiO_2	0.1	98.8	1.1
		spinel	7.7	0.2	92.1
103	1493 (1220)	liquid	7.9	34.6	57.5
		spinel	2.8	0.1	97.1
114	1493 (1220)	liquid	6.3	34.3	59.4
		spinel	2.8	0.5	96.7
115	1493 (1220)	liquid	15.2	35.0	49.8
		spinel	7.2	0.4	92.4
20	1523 (1250)	liquid	0.4	26.3	73.3
		spinel	0.1	0.0	99.9
62	1523 (1250)	liquid	2.4	34.7	63.0
		SiO_2	0.4	99.0	0.7
99	1523 (1250)	liquid	19.1	33.9	47.1
		spinel	9.3	0.4	90.3
100	1523 (1250)	liquid	12.7	34.2	53.1
		spinel	8.1	0.1	91.8
104	1523 (1250)	liquid	6.2	30.2	63.6
		spinel	3.5	1.1	95.4
113	1523 (1250)	liquid	1.6	26.3	72.1
		spinel	0.8	0.3	98.9
127	1523 (1250)	liquid	28.7	34.9	36.4
		spinel	14.7	0.3	85.0
128	1523 (1250)	liquid	0.8	25.9	73.3
		spinel	0.3	0.0	99.6
130	1523 (1250)	liquid	13.6	33.9	52.4
		spinel	7.3	0.5	92.2
126	1523 (1250)	liquid	0.2	36.4	63.5
		SiO_2	0.0	99.0	1.0
131	1523 (1250)	liquid	16.3	34.8	48.9
		SiO_2	0.4	98.8	0.8
111	1543 (1270)	liquid	0.7	21.2	78.1
		spinel	0.3	0.4	99.3
112	1543 (1270)	liquid	21.0	30.0	49.1
		spinel	10.1	0.4	89.5
123	1543 (1270)	liquid	28.8	32.1	39.1
		spinel	14.2	0.4	85.4
124	1543 (1270)	liquid	28.2	30.6	41.2
		spinel	14.4	0.3	85.3
133	1543 (1270)	liquid	16.6	35.8	47.7
		SiO_2	0.4	98.8	0.8
168	1543 (1270)	liquid	31.6	34.8	33.6
		spinel	17.7	0.3	82.0
		willemite	59.6	28.1	12.3
169	1543 (1270)	liquid	32.0	34.8	33.3
		spinel	17.9	0.3	81.8
		willemite	59.9	28.5	11.6
177	1543 (1270)	liquid	31.9	35.5	32.6
		willemite	59.8	28.5	11.6
		SiO_2	0.8	98.4	0.8
75	1573 (1300)	liquid	4.9	17.0	78.2
		wüstite	2.5	0.3	97.2
109	1573 (1300)	liquid	0.7	20.8	78.5
		spinel	0.2	0.4	99.4
134	1573 (1300)	liquid	1.6	15.5	82.9
		wüstite	1.0	0.3	98.8
140	1573 (1300)	liquid	28.0	26.6	45.3
		spinel	15.2	0.3	84.5

Table V. continued

Experiment No.	Temperature [K (°C)]	Phase	Composition (wt pct)		
			ZnO	SiO_2	"FeO"
144	1573 (1300)	liquid	6.8	18.7	74.5
		wüstite	3.5	0.4	96.0
145	1573 (1300)	liquid	34.9	31.8	33.3
		willemite	61.0	28.2	10.7
163	1573 (1300)	liquid	34.1	30.0	35.9
		spinel	18.3	0.3	81.3
		willemite	59.5	28.5	12.0
164	1573 (1300)	liquid	34.1	29.7	36.2
		spinel	18.9	0.3	80.8
171	1573 (1300)	liquid	37.0	35.8	27.2
		willemite	63.7	28.4	7.8
		SiO_2	1.1	98.2	0.6
173	1573 (1300)	liquid	30.9	29.3	39.8
		spinel	16.6	0.3	83.1
174	1573 (1300)	liquid	32.9	29.4	37.8
		spinel	16.2	0.3	83.5
180	1573 (1300)	liquid	16.2	36.5	47.3
		SiO_2	0.4	98.9	0.7
342	1573 (1300)	liquid	17.5	36.2	46.3
		SiO_2	0.3	98.9	0.8

determined 1523 K (1250 °C) isotherms at iron saturation[21] are also shown in the figure for comparison. The fully liquid area formed by the isotherms in different primary phase fields represents the operating range of the slag compositions at given temperature. It can be seen from the figure that the fully liquid area at 1523 K (1250 °C) determined in the present study is much smaller than that predicted by FactSage 6.2[29] which is almost same as the liquid region under metallic iron saturation.[21] Clearly the experimental results obtained in equilibrium with metallic iron cannot accurately predict the liquidus temperatures of ZnO-containing copper smelting slags. The database of FactSage 6.2 needs to be improved to accurately characterize the ZnO-containing copper smelting slags.

Different types of pseudo-binary phase diagrams are easy to be used by operators. Figure 8 presents a pseudo-binary diagram ("FeO" + SiO_2) − ZnO at fixed Fe/SiO_2 = 2 (mass) at Po_2 10^{-8} atm. Effect of ZnO on primary phases and liquidus temperatures is demonstrated in this figure. The predictions from FactSage 6.2[29] at Po_2 10^{-8} atm and that at metallic iron saturation[21] are also given in the figure for comparisons. It can be seen that spinel is the only primary phase with up to 30 wt pct ZnO as determined by the present study. The liquidus temperatures increase continuously with increasing ZnO. For instance, the liquidus temperature in the spinel phase field is increased by 35 K when ZnO content in liquid increases from 0 to 10 wt pct. At the same Po_2 10^{-8} atm, the liquidus temperatures predicted by FactSage 6.2[29] are much lower and willemite phase also appears at 25 wt pct ZnO. The experimentally determined phase diagram at metallic iron saturation[21] shows different primary phases and much lower liquidus temperatures.

To investigate the effect of fluxing condition represented by Fe/SiO_2 ratio, on the liquidus temperature in the ZnO-"FeO"-SiO_2 system, pseudo-binary phase diagram "FeO"-SiO_2 is constructed at fixed 5 wt pct ZnO as shown in Figure 9. The phase diagram of ZnO-free system at Po_2 10^{-8} atm and that at metallic iron saturation[21] are also given in the figure for comparisons. It can be seen from Figure 9 that the presence of 5 wt pct ZnO in the slag does not change the primary phase fields. The liquidus temperatures of the slag with 5 wt pct ZnO are generally higher in wüstite and spinel primary phase fields and lower in SiO_2 primary phase field than those of ZnO-free slag.

One of the advantages using EPMA technique is that the compositions of the solid phases can be measured simultaneously with the corresponding liquid phase. The partitioning of ZnO between liquid and solid is important to understand the thermodynamics of ZnO-containing slags. The partitioning of ZnO between spinel and liquid phases has been reported previously in the system ZnO-"FeO"-Al_2O_3-CaO-SiO_2 at metallic iron saturation.[24,30–34] The comparisons on the partitioning of ZnO between spinel and liquid at iron saturation, FactSage 6.2[29] predictions, and present study at Po_2 10^{-8} atm are shown in Figure 10. A linear relationship was found between ZnO in spinel phase and in liquid phase from present study and FactSage 6.2[29] predictions at Po_2 = 10^{-8} atm. The ZnO concentration in the spinel phase is approximately half of that in the liquid phase. The solubility of ZnO in the spinel determined in the present study is higher than that predicted from FactSage 6.2[29] which explains the reason for their difference on the liquidus temperatures.

The ZnO concentration in the spinel phase is much higher than that in liquid phase under metallic iron saturation as illustrated by the circles in Figure 10, which can be caused by Po_2 and/or slag compositions. In the present study (system ZnO-"FeO"-SiO_2), the spinel phase is a solid solution of $ZnFe_2O_4$ and Fe_3O_4. In the ZnO-"FeO"-Al_2O_3-CaO-SiO_2 system, the spinel

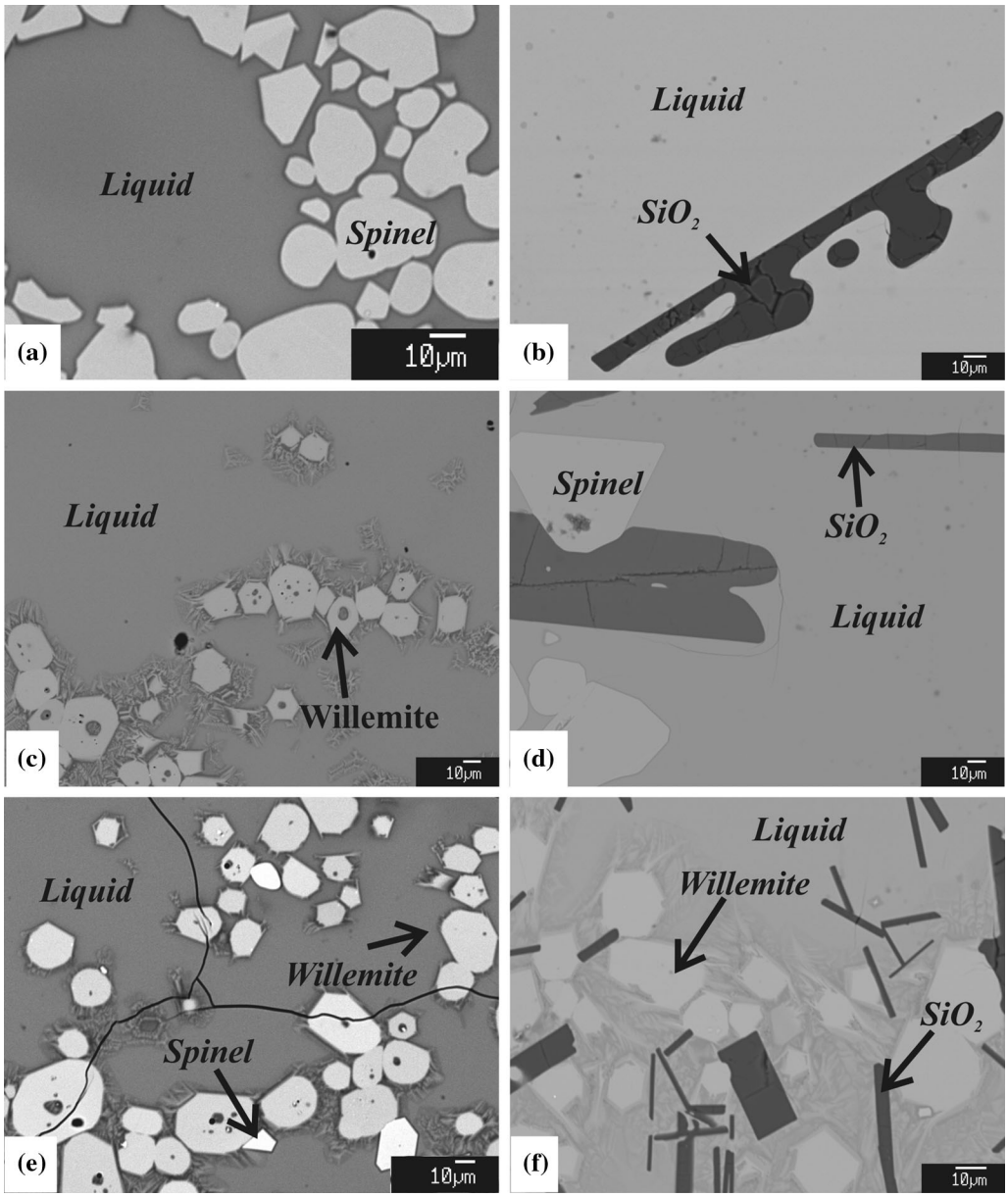

Fig. 5—Typical microstructures of the quenched samples in ZnO-"FeO"-SiO_2 system at Po_2 10^{-8} atm showing equilibrium of liquid with (*a*) spinel—1573 K (1300 °C); (*b*) tridymite—1543 K (1270 °C); (*c*) willemite—1573 K (1300 °C); (*d*) spinel + tridymite—1543 K (1270 °C); (*e*) spinel + willemite—1543 K (1270 °C); (*f*) tridymite + willemite—1543 K (1270 °C).

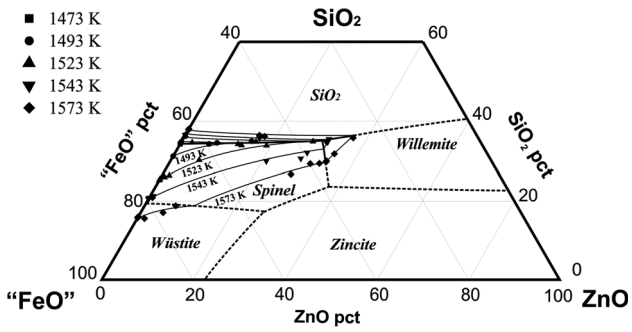

Fig. 6—Phase diagram with experimental data in ZnO-"FeO"-SiO_2 system at Po_2 10^{-8} atm.

phase is a solid solution of $ZnAl_2O_4$, $FeAl_2O_4$, $ZnFe_2O_4$, and Fe_3O_4. The Gibbs free energy of formation ($\Delta G_f°$) is −2247, −2181, −1462, and −1440 kJ mol^{-1} for $ZnAl_2O_4$, $FeAl_2O_4$, $ZnFe_2O_4$, and Fe_3O_4, respectively, at 1573 K (1250 °C) according to FactSage.[29] Clearly the Al_2O_3-containing compounds ($ZnAl_2O_4$ and $FeAl_2O_4$) are much stable than Al_2O_3-free compounds ($ZnFe_2O_4$ and Fe_3O_4). The accurate compositions of the spinel phase measured by EPMA enable the concentrations of the spinel-forming compounds to be calculated by mass balance. It has found that the concentrations of $ZnAl_2O_4$ and $FeAl_2O_4$ are much higher than that of $ZnFe_2O_4$ and Fe_3O_4 in the spinel phase under metallic iron saturation.[24,30–34] Effect of Po_2 on partitioning of

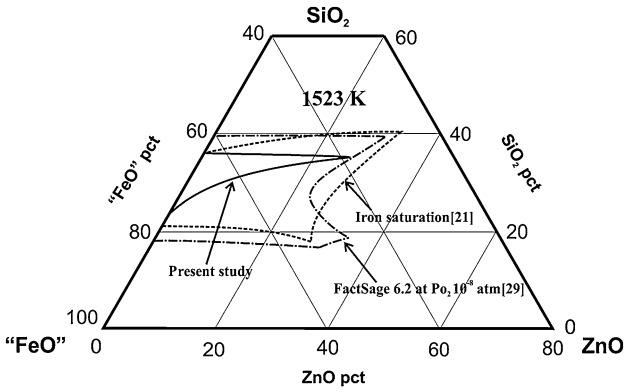

Fig. 7—Comparison of 1523 K (1250 °C) isotherms between the present study and FactSage 6.2[29] predictions on ZnO-"FeO"-SiO_2 system at Po_2 10^{-8} atm and metallic iron saturation.[21]

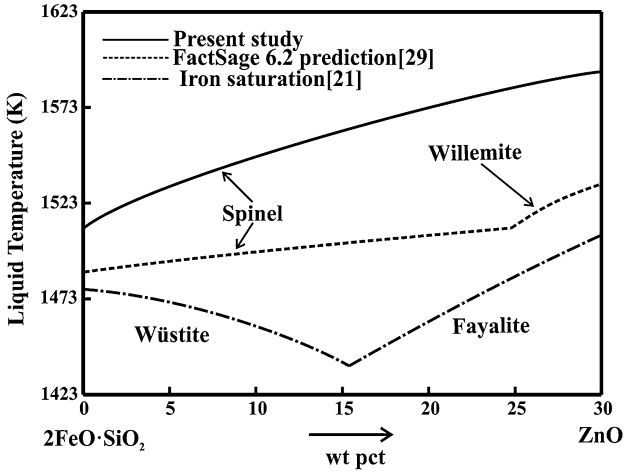

Fig. 8—Comparisons of pseudo-binary ("FeO" + SiO_2)-ZnO at fixed Fe/SiO_2 = 2 (mass) between present results and FactSage predictions[29] at Po_2 10^{-8} atm, and also that at iron saturation.[21]

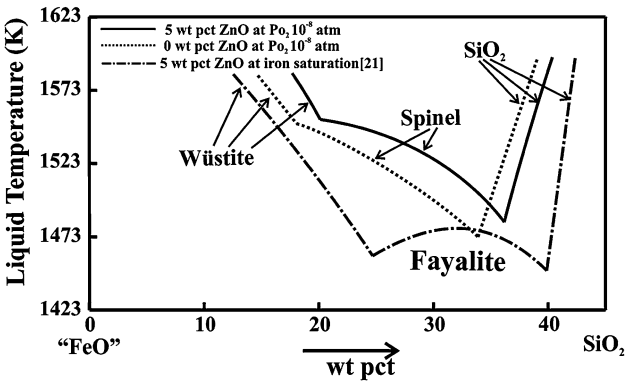

Fig. 9—Pseudo-binaries "FeO"-SiO_2 at fixed 0 and 5 wt pct ZnO at Po_2 at 10^{-8} atm and iron saturation.[21]

Zn to spinel will be evaluated when the data in the system ZnO-"FeO"-Al_2O_3-SiO_2 at Po_2 10^{-8} atm are available.

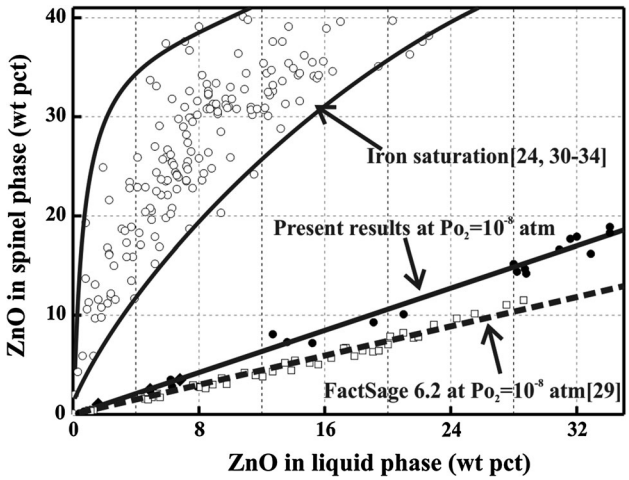

Fig. 10—Comparison of partitioning effect of ZnO between liquid phase and spinel phase, from current experiments, Factsage prediction,[29] and results under metallic iron saturation.[24,30–34]

IV. CONCLUSIONS

Phase equilibrium studies have been conducted at oxygen partial pressure 10^{-8} atm relevant to copper smelting conditions in the temperature range from 1473 K to 1573 K (1200 °C to 1300 °C). The liquidus temperatures and primary phase fields in the "FeO"-SiO_2 and ZnO-"FeO"-SiO_2 systems have been experimentally determined. The liquidus temperatures obtained from the present study in spinel primary phase field are higher than that predictions by FactSage 6.2 and that measured at metallic iron saturation. The liquidus temperatures in spinel primary phase field increase with increasing ZnO concentration in slag. ZnO partitioning between spinel phase and liquid phase has been compared at Po_2 = 10^{-8} atm and metallic iron saturation. The findings in the present study fill the knowledge gap of Zn-containing system relevant to copper smelting slags, and have direct implications to the industrial operations.

ACKNOWLEDGMENTS

The authors wish to thank Dongying Fangyuan Nonferrous Metals Co., Ltd. and The University of Queensland for providing the financial support to enable this research to be carried out; The University of Queensland International Research Tuition Award (UQIRTA) and China Scholarship Council (CSC) for providing scholarships for Hongquan Liu; and Mr. Ron Rasch and Ms Ying Yu of the Centre for Microscopy and Microanalysis at the University of Queensland, who provided technical support for the EPMA facilities.

REFERENCES

1. M.E. Schlesinger, M.J. King, K.C. Sole, and W.G.I. Davenport: *Extractive Metallurgy of Copper*, Elsevier, Oxford, 2011.

2. M. Chen, S. Raghunath, and B.J. Zhao: *Metall. Mater. Trans. B*, 2013, vol. 44B, pp. 820–27.
3. B. Zhao, Z. Cui, and Z. Wang: *4th International Symposium on High-Temperature Metallurgical Processing*, Wiley. 2013, pp. 1–10.
4. M. Chen, Z. Cui, and B. Zhao: *6th International Symposium on High-Temperature Metallurgical Processing*, Wiley. 2015, pp. 257–264.
5. Z. Cui, Z. Wang, and B. Zhao: *Copper 2013: Copper International Conference*. 2013, pp. 923–933.
6. R. Hansson, B. Zhao, P.C. Hayes, and E. Jak: *Metall. Mater. Trans. B*, 2005, vol. 36B, pp. 187–93.
7. E.N. Bunting: *J. Am. Ceram. Soc.*, 1930, vol. 13, pp. 5–10.
8. R. Hansson, P.C. Hayes, and E. Jak: *Trans. Inst. Min. Metall., Sect. C*, 2005, vol. 114, pp. 141–46.
9. R. Hansson, P. Hayes, and E. Jak: *Metall. Mater. Trans. B*, 2005, vol. 36B, p. 7.
10. R. Hansson, P.C. Hayes, and E. Jak: *Scand. J. Metall.*, 2004, vol. 33, pp. 294–304.
11. S. Itoh, K. Sato, S. Nakazawa, and T. Azakami: *Shigen Sozai*, 1989, vol. 105, pp. 739–43.
12. S. Itoh and T. Azakami: *Mater. Trans., JIM*, 1995, vol. 36, pp. 1074–80.
13. S. Itoh and T. Azakami: *Nippon Kinzoku Gakkaishi*, 1994, vol. 58, pp. 1288–93.
14. N.L. Bowen and J.F. Schairer: *Am. J. Sci. Ser. 5*, 1932, vol. 24, pp. 177–213.
15. A. Muan: *Am. J. Sci.*, 1958, vol. 256, pp. 171–207.
16. A. Muan: *Trans. AIME J. Met.*, 1955, vol. 7, pp. 965–76.
17. T. Hidayat, P. Hayes, and E. Jak: *Metall. Mater. Trans. B*, 2012, vol. 43B, pp. 27–38.
18. L.S. Darken: *J. Am. Chem. Soc.*, 1948, vol. 70, pp. 2046–53.
19. E. Jak, S. Degterov, A.D. Pelton, and P.C. Hayes: *Metall. Mater. Trans. B*, 2001, vol. 32B, pp. 793–800.
20. E. Jak, B. Zhao, and P. Hayes: *Metall. Mater. Trans. B*, 2000, vol. 31B, pp. 1195–201.
21. B. Zhao: *Phase Equilibria for Copper Smelting and Lead/Zinc Reduction Slags*, University of Queensland, Brisbane, 1999.
22. S. Itoh and T. Azakami: *Shigen Sozai*, 1993, vol. 109, pp. 325–29.
23. M. Chen and B. Zhao: *J. Am. Ceram. Soc.*, 2013, vol. 96, pp. 3631–36.
24. B. Zhao, P.C. Hayes, and E. Jak: *Int. J. Mater. Res.*, 2011, vol. 102, pp. 134–42.
25. B. Zhao, P. Hayes, and E. Jak: *J. Min. Metall. Sect. B.*, 2013, vol. 49, pp. 153–59.
26. H.M. Henao and K. Itagaki: *Metall. Mater. Trans. B*, 2007, vol. 38B, pp. 769–780.
27. E. Jak and P.C. Hayes: *Trans. Inst. Min. Metall., Sect. C*, 2008, vol. 117, pp. 1–17.
28. R.A. Mendybaev, J.R. Beckett, E. Stolper, and L. Grossman: *Geochim. Cosmochim. Acta*, 1998, vol. 62, pp. 3131–39.
29. C.W. Bale, E. Bélisle, P. Chartrand, S.A. Decterov, G. Eriksson, K. Hack, I.H. Jung, Y.B. Kang, J. Melançon, A.D. Pelton, C. Robelin, and S. Petersen: *CALPHAD: Comput. Coupling Phase Diagr. Thermochem.*, 2009, vol. 33, pp. 295–311.
30. B. Zhao, P.C. Hayes, and E. Jak: *Int. J. Mater. Res.*, 2011, vol. 102, pp. 269–76.
31. B. Zhao, P.C. Hayes, and E. Jak: *Metall. Mater. Trans. B*, 2011, vol. 42B, pp. 490–99.
32. B. Zhao, P.C. Hayes, and E. Jak: *Metall. Mater. Trans. B*, 2011, vol. 42B, pp. 50–67.
33. B. Zhao, P.C. Hayes, and E. Jak: *Metall. Mater. Trans. B*, 2010, vol. 41B, pp. 386–95.
34. B. Zhao, P.C. Hayes, and E. Jak: *Metall. Mater. Trans. B*, 2010, vol. 41B, pp. 374–85.